

Section method for monitoring the surface shape of a radiation spot in real time

Leonid Tymchenko, Natalia Kokriatska, Volodymyr Tverdomed, Yurii Kutaev, Dmytro Zhuk
 Department of Telecommunication Technologies and Automation
 State University of Infrastructure and Technology
 Kyiv, Ukraine
 zhuk_do@ukr.net

Abstract— An approach to solving the problem of monitoring the surface shape of a radiation spot in real life. The analysis of the use of the section method for monitoring the shape of the surface of the radiation spot in real time is carried out. Considered the possibility of using aspect ratio to solve a given problem. Experimental studies of the method of sections and form factor.

Keywords— section method; radiation spot; surface shape; laser beam paths.

I. INTRODUCTION

Currently, in printing, laser processing of materials, location, optical communication and other fields of technology there is a need for wider implementation of optoelectronics systems with automatic correction of distortions of light radiation that is formed. The causes of these distortions can be the destabilizing effect of mechanical or climatic factors, instability of the characteristics of the radiation source, perturbations in the optical path, misalignment of optical elements, etc. Ensuring acceptable correction quality requires continuous dynamic monitoring of the characteristics of light radiation, such as the spatial distribution of its intensity, including the assessment of the deviation of the specified distribution from the original or reference distribution.

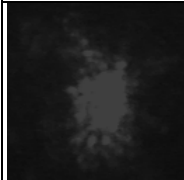
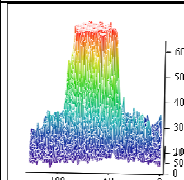
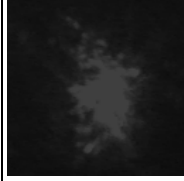
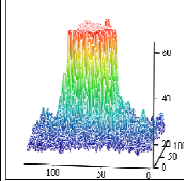
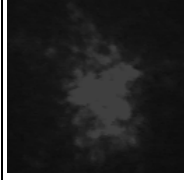
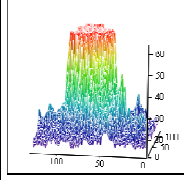
In comparison with previous works in this article was offered the method of sections on which it is possible to carry out classification of images of spots of laser beams and other images.

The aim of the article is to develop a cross-section method for control of the surface form of a radiation spot in real time.

II. APPROXIMATE CLASSIFICATION FUNCTION

The traditional way to solve this problem involves forming an image of the radiation spot $B(x, y)$ on the light-sensitive surface of the photodetector, followed by conversion into a signal $U(x, y)$, the amplitude of which at each decomposition point with coordinates (x, y) corresponds to the intensity in $B(x, y)$, that is $U(x, y) \leftrightarrow B(x, y)$. The example of such conversion is shown in Table 1.

TABLE I. CONVERSION OF RADIATION SPOT INTO A SIGNAL .

Laser spot	Graph of the laser spot	Shape coefficient	Spot focusing parameter
		$B = 0.766$	$q = 2.123$
		$B = 0.766$	$q = 2.116$
		$B = 0.756$	$q = 2.069$

Next, the signal $U(x, y)$ is compared with the reference signal $W(x, y)$ for all decomposition points of the signals. The signals $U(x, y)$ and $W(x, y)$ are some surfaces that may differ in type, relative scale factor, relative coordinate reference vector, and relative rotation angles in three-dimensional space. Therefore, the comparison of these surfaces should be made taking into account all possible situations, which requires a huge amount of computation and is quite difficult to implement in real time.

In practically important cases, the necessary comparison of the surfaces $U(x, y)$ and $W(x, y)$ can be realized using the following new method of intersections. This method includes

the following operations [1]:

- finding the maximum amplitudes of the signals $U(x, y)$ and $W(x, y)$ (Fig. 1)

$$U_{\max} = \max U(x, y) = h_u \quad (1)$$

$$W_{\max} = \max W(x, y) = h_w \quad (2)$$

- finding the values of areas $S_{0,75u}$ and $S_{0,5u}$ sections at $0,75h_u$ and $0,5h_u$ the levels of for the signal $U(x, y)$, respectively $S_{0,75w}$ and $S_{0,5w}$ at the levels of $0,75h_w$ and $0,5h_w$ for the signal $W(x, y)$ respectively;
- calculation of approximate values of form coefficients $\tilde{r}_{v,u}$ and $\tilde{r}_{v,w}$ for signals $U(x, y)$ and $W(x, y)$ respectively;

$$r_{v,u} \approx \tilde{r}_{v,u} = r_{s,u} = S_{0,75u} / S_{0,5u} \quad (3)$$

$$r_{v,w} \approx \tilde{r}_{v,w} = r_{s,w} = S_{0,75w} / S_{0,5w} \quad (4)$$

where \sim is the sign of the approximate value,

$$r_{v,u} = V_{0,5u} / h_u S_{0,5u}, \quad 0 < r_{v,u} \leq 1 \quad (5)$$

$$r_{v,w} = V_{0,5w} / h_w S_{0,5w}, \quad 0 < r_{v,w} \leq 1 \quad (6)$$

$V_{0,5u}$ and $V_{0,5w}$ - the total value of the amplitudes of the signals $U(x, y)$ and $W(x, y)$, lower levels of $0,5h_u$ and $0,5h_w$, respectively;

- comparison of form coefficients $r_{s,u}$ and $r_{s,w}$ (instead of element-by-element comparison of surfaces).

We show the validity $r_v \approx r_s$ of the example of the current signal $U(x, y)$ as follows.

The volume $\tilde{V}_{0,5u}$ of the figure above the cross section of the surface $U(x, y)$ at the level of $0,5h_u$ can be found using one of the known formulas for approximate calculation of integrals for equidistant nodes, for example, the Simpson

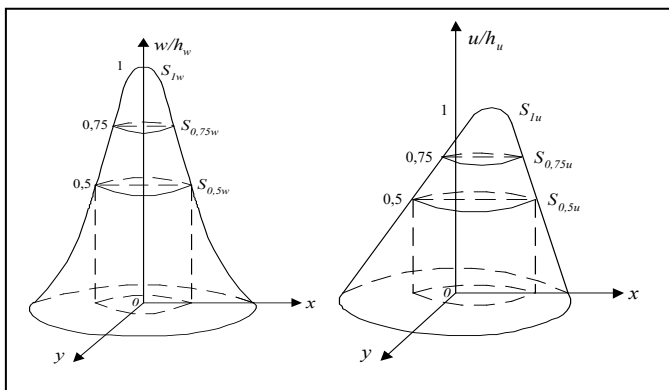


Fig. 1. - Signals of the reference and current images of the radiation spot.

formula:

$$\tilde{V}_{0,5u} \approx h_u [S(U_{\max}) + 4S_{0,75u} + S_{0,5u}] / 12 \approx h_u S_{0,5u} (4r_{s,u} + 1) / 12 \quad (7)$$

since $S(U_{\max}) = S_{1u}$ is the cross-sectional area of the surface at the level of the maximum amplitude, most often $S_{1u} \approx 0$.

Using (7) is easy to obtain

$$V_{0,5u} = \tilde{V}_{0,5u} + h_u S_{0,5u} / 2 \approx h_u S_{0,5u} (4r_{s,u} + 7) / 12 \quad (8)$$

from where it follows

$$\tilde{r}_{v,u} \approx (4r_{s,u} + 7) / 12 \quad (9)$$

The linear dependence of the coefficients \tilde{r}_v and r_s allows you to use the coefficient r_s as a characteristic of the shape of the corresponding surface [2].

Possibilities of classification of types of surfaces by means of factor r_s are shown in the Table 2. Different values of the coefficient r_s correspond to different types of surfaces of the examples of figures given in it.

An important advantage of the coefficient r_s for some types of surfaces is its independence from the coefficient of scale, displacement and orientation on the corresponding surface. In addition, the calculation of the coefficient r_s , since the number of bits of the value code $S_{0,5}$ is always significantly less than the number of bits of the value code $V_{0,5}$.

The coefficient $4r_s$ characterizes the generalized convexity of the surface: when $4r_s > 1$ - the surface is convex, when $4r_s < 1$ the surface is flat in the generalized sense, when $4r_s = 1$ - the surface is linear in the generalized sense.

It is important to note that the surface can be characterized by the effective cross-sectional area S_3 :

$$S_3 = 2(V_{0,5} - S_{0,5} \cdot h \cdot 0,5) / h \approx 2(S_{0,5} \tilde{r}_v h - S_{0,5} \cdot h \cdot 0,5) / h = 2S_{0,5}(\tilde{r}_v - 0,5) \quad (10)$$

from which it follows

$$S_3 \approx \tilde{S}_3 = \begin{cases} (4S_{0,75} + S_{0,5}) / 6 & \text{при } S_1 \approx 0, \\ (S_1 + 4S_{0,75} + S_{0,5}) / 6 & \text{при } S_1 \neq 0, \end{cases} \quad (11)$$

Where S_1 is the cross-sectional area of the signal at its maximum level.

From the aspect ratio \tilde{r}_v , it is easy to generate the focusing parameter of the emission spot:

$$q_\phi \sim \frac{h}{\sqrt{S_3}} \sim \frac{h}{\sqrt{S_{0,5}(\tilde{r}_v - 0,5)}} \quad (12)$$

According to the presented method, it is necessary to adapt the surface to the extent that it is possible to adapt it in terms of efficiency and not to the extent to which it is possible to adapt it to all types of factors. It is important to note that the equivalence of the characteristics of the surface form, allowing to bring them to one of the same general type of surface or an approximate type of surface.

Obviously, the section method can easily be stuck in the case of an increase in the number of sections on the surface, or changes in the value of sections, changes in the performance of the section areas [3].

At the same time, in terms of quality, the basis is also partially victorious, using an approximate formula for the approximate calculation of integrals.

The section method can easily be extended to the effect of increasing the number of section surfaces, or changing the value of sections, changing the performance of section areas. At the same time, in terms of the nature of the basis, the basis is also subtly use the formulas for the approximate calculation of integrals. The method of recollection is promising as well for storing in problems of classification and archivation of images in real time. An important experience of the given method is the simplicity of working with both software and hardware [4-7].

The cross section method [8] can be used for sampling of laser beam signals (Fig. 3), and the shape coefficient can be used as a sampling parameter. At the same time, this technique will be used to find the centers of the laser beams. This is one of the main problems while processing laser beam spots for atmospheric optical communication systems, along with the image classification with aim to remove overly noisy (distorted) images.

The algorithm is as follows:

1. There is a dot with maximum brightness in the image.
2. From the found brightness value in the image, five brightness values are selected, each one less than the previous one. The endpoints of each of the six ranges form boundary lines. The result is six boundary lines.
3. For each edge contour, a preliminary center is determined, after which the averaged center for the X and Y coordinates is calculated.

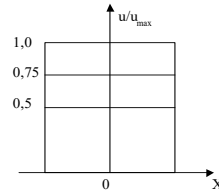
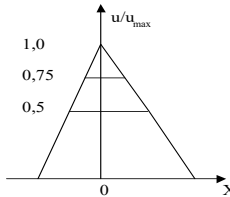
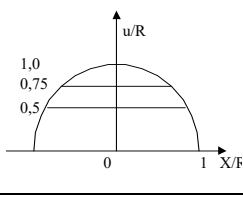
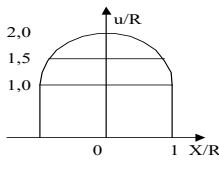
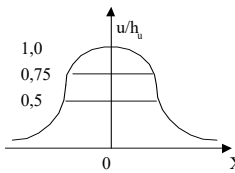
The coordinates (x, y) of the energy center of a two-dimensional signal with a specific nonlinear density $w(f(x,y))$ corresponding to a given value of $f(x, y)$ are expressed as follows:

$$x = \frac{1}{M} \sum_{x=0}^{N-1} \sum_{y=0}^{N-1} w(f(x,y))x \quad (13)$$

$$y = \frac{1}{M} \sum_{x=0}^{N-1} \sum_{y=0}^{N-1} w(f(x,y))y \quad (14)$$

$$M = \sum_{x=0}^{N-1} \sum_{y=0}^{N-1} w(f(x,y)) \quad (15)$$

TABLE II. POSSIBILITIES OF CLASSIFICATION OF TYPES OF SURFACES BY MEANS OF FACTOR .

Longitudinal section drawing	Coefficient values			Error value
	r_s	\tilde{r}_y	r_y	
1. Prism, cylinder 	1	$\frac{11}{12} \approx 0.92$	1	$\frac{1}{12} \approx 0.083$
2. Pyramid, cone 	$1/4=0.25$	$\frac{2}{3} \approx 0.67$	$\frac{2}{3} \approx 0.67$	0
3. Hemisphere 	$\frac{7}{12} \approx 0.58$	$\frac{7}{9} \approx 0.78$	$\frac{7}{9} \approx 0.78$	0
4. Hemisphere with base 	$\frac{3}{4} \approx 0.75$	$\frac{5}{6} \approx 0.83$	$\frac{5}{6} \approx 0.83$	0
5. Gaussoid $(1/\sqrt{2\pi}) \exp\{-(x^2+y^2)/2\}$ 	$\frac{\ln(4/3)}{\ln 2} \approx 0.415$	$\frac{8.66}{12} \approx 0.722$	$\frac{1}{2 \ln} \approx 0.721$	≈ 0

4. The resulting edge lines are divided into four segments. The coordinates of the preliminary center (averaged center) are used as the central point.
5. Determine the "good" and "bad" images upon entering the calculated tunnel of the calculated form factor.

If the shape ratio of the image enters the tunnel, the latter is considered "good", otherwise - "bad".

The boundaries of the tunnel are calculated in the

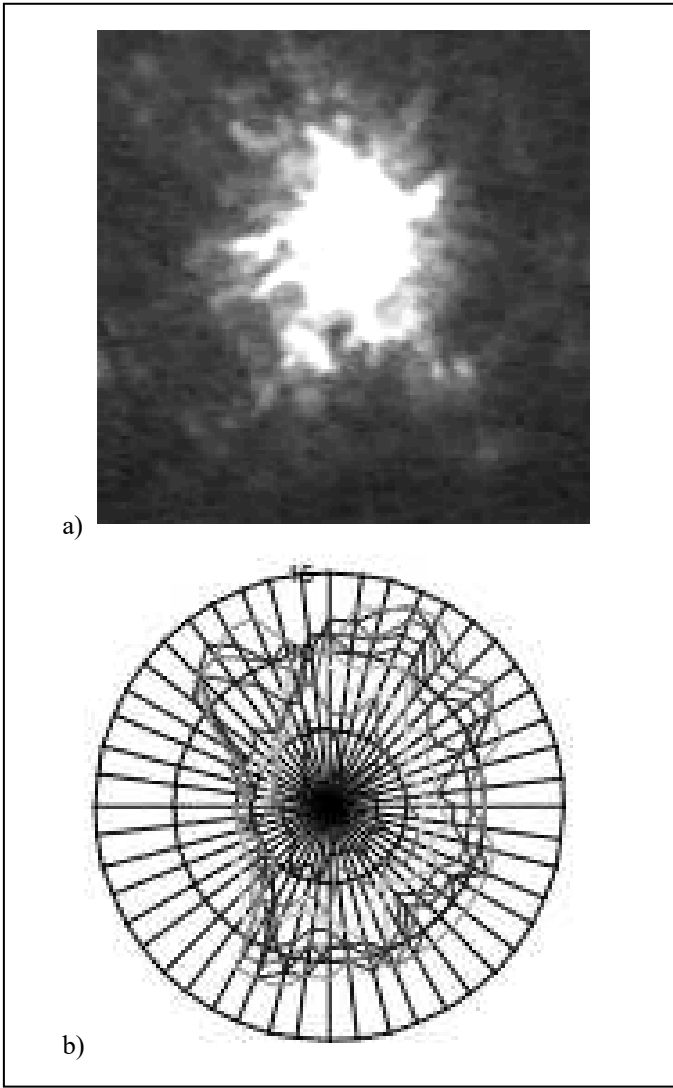


Fig. 2 – The shape of the spot of the laser beam: a - photo from the camera; b - schematic drawing

trained sample of images by sequential selection of images and the corresponding form coefficients with a minimum scatter of the coordinates of the preliminary centers.

6. The coordinates of energy centers are calculated only for "optimal" images.

III. EXPERIMENTAL PART

There were studied 15 laser beam paths [9] and the following results were obtained (shown for two paths):

- Tunnel boundaries

$$a := 0.777, b := 0.78 \quad (16)$$

The value of the difference between the maximum and minimum value of the coordinates is 1,147.

The diagram of the distribution of the coordinates of the centers of the laser beams for given boundaries are showed on Fig. 3.

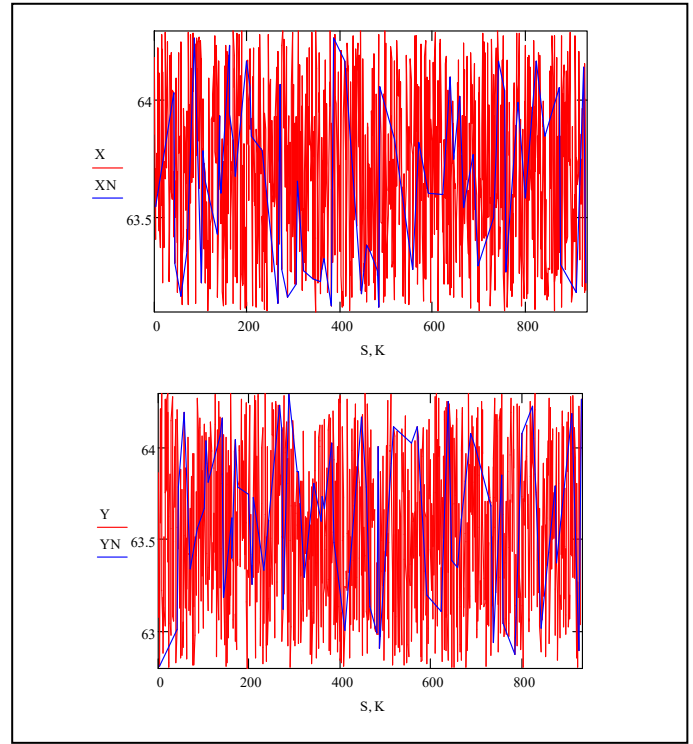


Fig. 3. - Diagram of the distribution of the coordinates of the centers of the laser beams, where X, the coordinates of the entire path of the laser beams XN is the value of the coordinates of the centers of the spots after sampling.

- Tunnel boundaries

$$a := 0.751, b := 0.757 \quad (17)$$

The value of the difference between the maximum and minimum coordinate values is 2.18.

The diagram of the distribution of the coordinates of the centers of the laser beams for the last given boundaries are showed on Fig. 4.

For the diagram on Fig. 3 the boundaries are:

$$a := 0.777, b := 0.78 \quad (18)$$

The difference between *min* and *max* for coordinate X is:

$$\max(XN) - \min(XN) = 1.147 \quad (19)$$

for Y:

$$\max(YN) - \min(YN) = 1.476 \quad (20)$$

For the diagram on Fig. 4 the boundaries are:

$$a := 0.751, b := 0.757 \quad (21)$$

The difference between *min* and *max* for coordinate X is:

$$\max(XN) - \min(XN) = 2.18 \quad (22)$$

for Y:

$$\max(YN) - \min(YN) = 1.476 \quad (23)$$

Comparative analysis shows that the proposed methods make it possible to measure the coordinates of the center of laser images with an accuracy of determining the anchor point of at least 1–2 decomposition elements, which in accuracy exceeds the known ones, for example, based on the determination of the center of mass using moment signs, on average in 1.5 times.

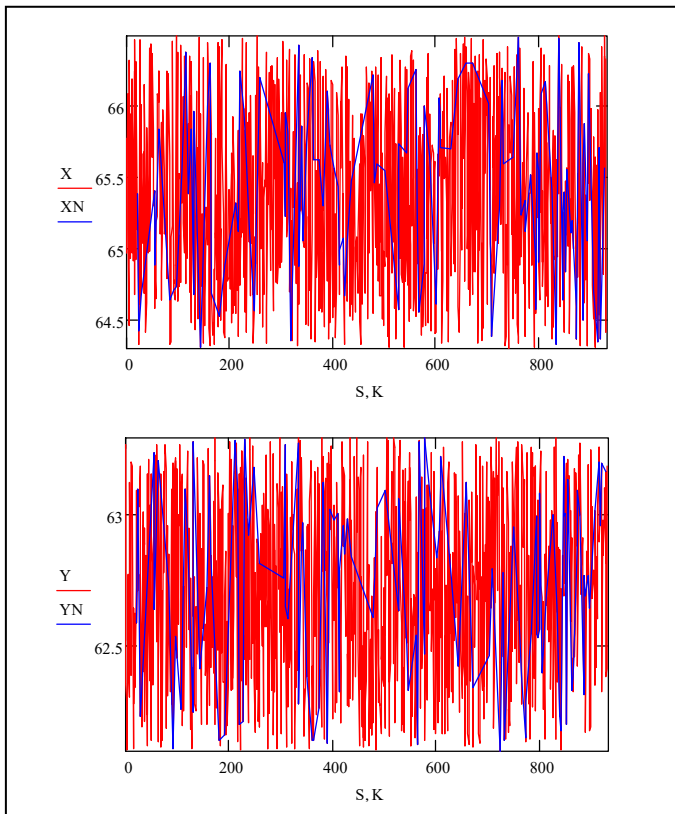


Fig. 4. - Diagram of the distribution of the coordinates of the centers of the laser beams, where X, the coordinates of the entire path of the laser beams XN is the value of the coordinates of the centers of the spots after sampling.

IV. CONCLUSIONS

With the help of experiments, it can be said that for images of radiation spots as a result of the action of various unfavorable factors, it is impossible to accurately measure the coordinates of their energy centers, however, the accuracy can be significantly increased using the calculation of the shape factor of the images with their subsequent classification.

It is important to note that the equality of the shape coefficients of surfaces in the general case allows them to be attributed to the same generalized type of surface or approximated by this type of surface.

When using the presented method of sections, the comparison of surfaces is reduced to comparing their shape coefficients and does not require element-by-element comparison, taking into account all cases of differences in their types, scale factor, relative shift and rotation in space.

This method can be effectively used in systems that work with laser beam signals. Those are: laser beam profiling systems used in medicine and materials processing, where it is necessary to control the position of the energy center and the size of the laser beam spot; fiber optic communication systems to control the alignment of equipment; systems of laser navigation and tracking of objects in military affairs and atmospheric-optical communication lines, in which it is

necessary to determine the direction of beam displacement. Such tasks are primarily reduced to determining the energy center, i.e. the coordinates of the center of gravity of the images of the laser beam and determining its contour, which can be implemented using the considered in this study method.

These tasks are especially important for atmospheric-optical laser communication systems, where due to atmospheric phenomena the trajectory of the laser beam is constantly shifted, and the laser beam itself undergoes significant defects, resulting in getting a large error (up to 10 dimensional elements) while getting coordinates of its center. Accurate positioning requires the use of additional methods, including processing the contour of the laser spot. Given the inertia of positioning systems, it is necessary to know not only the existing position of these devices, but also to be able to predict it with some probability.

The considered method is also useful for application in problems of classification and archiving of images in real time [10, 11]. The advantage of this method is the ease of implementation, both software and hardware.

REFERENCES

- [1] L. Tymchenko, M. Petrovskiy, N. Kokriatska, V. Gubernatorov and Y. Kutaev, "Modeling of the high-performance PLD-based sectioning method for classification of the shape of optical object images", SpringerPlus volume 2, Article number: 692 (2013).
- [2] A. Polyinin, A. Chernoutsan, "A Concise Handbook of Mathematics, Physics, and Engineering Sciences", 2017.
- [3] A. Mishin, "Method, algorithm and adaptive processing device images based on CMOS video sensors using neuro-like structures" 2015, pp. 9 - 33.
- [4] L. Timchenko, Y. Kutaev, A. Gertsiy, "System Coordinate Reference for Nonstationary Signals", 2001, No. 6, pp. 886-890.
- [5] L. Timchenko, P. Pijarski, V. Zavadskiy, S. Nakonechna, N. Kokriatska, "Processing laser beam spot images using the parallel-hierarchical network for classification and forecasting their energy center coordinates" Proc. SPIE 10031, Photonics Applications in Astronomy, Communications, Industry, and High-Energy Physics Experiments, 2016, September 2016.
- [6] K. Nobuo, O. Hitoshi, N. Satoru, "Surface shape measurement apparatus, surface shape measurement method, surface state graphic apparatus", 2007, p. 64.
- [7] L. Tymchenko, V. Tverdomed, N. Kokriatska, N. Petrovsky, "Development of a method of processing images of laser beam bands with the use of parallel hierarchic networks", Eastern-European Journal of Enterprise Technologies, vol 9, 2019, pp. 21-27.
- [8] Y. Kutaev, A. Sidorov, "Method for filtering geometric noise of a binary image", Collection of scientific works "Information and microprocessor technology in the printing industry", 1992, pp. 57-73.
- [9] N. Basov, E. Zemskov, Y. Kutaev, "Laser Control of Near Earth Space and Possibilities for Removal of Space Debris from Orbit with Explosive Photo-Dissociation Lasers with Phase Conjugation", 1998, pp. 156-158.
- [10] A. Yarovyvy, L. Tymchenko, N. Kokriatska, "Parallel-Hierarchical Computing System for Multi-Level Transformation of Masked Digital Signals", Advances in Electrical and Computer Engineering, vol. 12, Number 2012.
- [11] L. Tymchenko, N. Kokriatska, A. Gertsiy, A. Kotyra, Y. Amirgaliyev, "Elaboration of pyramidal methods applying computation technique rough-fine image identification", Proceedings of SPIE - The International Society for Optical Engineering. 2019.